Decoherence of coherent transport in a disordered one-dimensional wire: Phenomenological model

Martin Moško*
Institute of Electrical Engineering, Slovak Academy of Sciences, Dúbravská cesta 9, 842 39 Bratislava, Slovakia

Pavel Vagner
Institut für Schichten und Grenzflächen, Forschungszentrum Jülich GmbH, 52425 Jülich, Germany and
Institute of Electrical Engineering, Slovak Academy of Sciences, Dúbravská cesta 9, 842 39 Bratislava, Slovakia

Peter Markoš
Institute of Physics, Slovak Academy of Sciences, Dúbravská cesta 9, 842 28 Bratislava, Slovakia

Thomas Schäpers
Institut für Schichten und Grenzflächen, Forschungszentrum Jülich GmbH, 52425 Jülich, Germany

(Dated: February 1, 2008)

We model the effect of phase-breaking collisions on the coherent electron transport in a disordered one-dimensional single-channel wire. In our model the phase-breaking collisions break the wire into segments, where each segment is an independent series resistor with coherent electronic resistance and the segmentation is a stochastic process with Poisson distribution of phase-breaking scattering times. The wire resistance as a function of the wire length L, coherence length L_ϕ, and localisation length ξ is calculated and the transition from coherent to incoherent transport is traced quantitatively. In the coherent regime ($L < L_\phi$) the resistance fluctuates from wire to wire with a characteristic log-normal distribution of resistances, the typical resistance increases as $\exp(L/\xi)$, and the mean resistance increases as $\exp(2L/\xi)$ (or faster if disorder is strong). As L exceeds L_ϕ, decoherence suppresses the resistance fluctuations and narrows the resistance distribution. As a result, at $L \gg L_\phi$ the mean resistance increases as $\beta L - c$ and the typical resistance as $\beta L - c'$, where β is the wire resistivity, c is a constant shift due to the decoherence near the source electrode, and $c' \gg c$ is the shift related to the resistance self-averaging in a single wire. Numerical results are given for a GaAs quantum wire. It is noted that coherent transport in such wire can exhibit peculiar deviations from universal scaling owing to strong backscattering by impurities.

PACS numbers: 73.23.-b, 73.61.Ey

I. INTRODUCTION

Electron gas confined in a GaAs quantum wire is a realistic one-dimensional (1D) electron gas system that almost ideally manifests (or is expected to manifest) a variety of fundamental 1D transport effects.[1]

If the wire is much shorter than the electron mean free path, electron transport is ballistic. Then each energy subband occupied by the 1D electrons contributes to the wire conductance by an amount $2e^2/h$, i.e., the conductance is universally quantized and wire-length-independent.[2,3] This effect is explained by the Landauer conductance formula[4,5,6] if one considers just ballistic transport of non-interacting 1D electrons. Incorporation of many-body effects gives the same result.[7]

Disorder affects the 1D transport in a complicated way. Consider first the model of non-interacting coherent electrons. A coherent 1D electron wave in a disordered 1D wire of infinite length is exponentially localized by an arbitrary weak disorder[8,9] (it does not exhibit Anderson transition[10]). The resistance of a finite 1D wire should therefore increase exponentially with the wire length. In fact, the resistance wildly fluctuates from wire to wire in an ensemble of macroscopically identical wires (because disorder in each wire is microscopically different) and what increases exponentially is the average resistance.[4,11] A full distribution of resistances in the ensemble of weakly disordered 1D wires is given by the Dorokhov-Mello-Pereyra-Kumar (DMPK) equation – an important result of the scaling theory of localization.[12]

How are these localization effects modified by many-body interactions? As discussed below, this is an open question especially for a single-channel 1D wire.

Authors of Ref. 13 considered tunneling of the interacting 1D electron gas through a single impurity and examined how the many-body interaction renormalizes single-particle tunneling. They found at zero temperature, that the 1D electron at the Fermi level is perfectly reflected by Friedel oscillations of the Hartree-Fock many-electron potential around the impurity. Thus, the impurity is impenetrable and the zero temperature conductance is zero.

However, for such perfect reflection an infinitely long tail of Friedel oscillations is needed. Therefore, a single impurity in the wire of finite length still exhibits a nonzero (albeit reduced) penetrability.[13] Many impurities distributed at random along the finite-length wire can thus be expected to cause a similar (exponential) localization as in the case of non-interacting gas.

So far we have discussed coherent transport. Indeed, localization and Friedel oscillations are due to the interference of incident and reflected electron waves, for which electron coherence is needed. However, the electron-electron (e-e) interaction in general causes also the phase-breaking e-e collisions and thus acts against interference. Recent theories of the e-e interaction mediated phase breaking[14,15] are applicable to a quasi-1D (multichannel) wire, not to the 1D quantum wire with a single conducting channel. The same can be said about experiments[16,17] in which the phase breaking is detected from magnetotransport in weakly localized regime.

The e-e interaction mediated phase breaking in the 1D quantum wire should in principle be tractable within the Landauer conductance formulation (see the discussion in Sect. IV). Various Landauer-type formulations were used to analyze the effect of point-like phase breakers placed at fixed positions in a random chain of elastic scatterers (e.g. Refs. 18 and 19), but the phase breaking by e-e interaction was not considered.

Authors of Refs. 20 and 21 considered two interacting electrons moving in disorder and found that the electron localization length is enhanced in comparison with the single-electron situation. Obviously, the phase breaking is not identified in this approach as the interference (exponential localization) still exists. The phase breaking which destroys exponential localization can perhaps arise in the analysis involving many interacting 1D particles: The many-particle interaction redistributes energy in a clean 1D electron system,[22,23] so perhaps this inelastic process persists also in a disordered 1D system.

Such many-particle analysis is a formidable problem, but a few interesting questions can be addressed within a simple phenomenological model developed in this work. In particular, as already mentioned, coherent transport in a weakly disordered 1D wire is described by the DMPK equation,[12] which determines the distribution of resistances in the ensemble of macroscopically identical wires (eq. 6). We want to show how the phase-breaking collisions, if any, modify the DMPK distribution and the mean and typical resistance related to this distribution.

We examine transport in a disordered 1D wire with a single conducting channel, specifically in the ground subband of a GaAs quantum wire. Our model is in essence a simple phenomenological model of the e-e interaction mediated phase breaking, with the electron coherence length treated as a parameter. In the model the phase-breaking collisions effectively break the wire into independent segments, where each segment is a series resistor with coherent electron motion. We model the segmentation as a stochastic process with a Poisson distribution of phase-breaking scattering times and evaluate the resistance of each segment microscopically from the Landauer formula.

The wire resistance as a function of the wire length L, coherence length L_ϕ, and localisation length ξ is traced from the coherent regime at $L < L_\phi$ up to the incoherent one at $L \gg L_\phi$. We find the following results.

In the coherent regime the resistance fluctuates from wire to wire in accord with the DMPK resistance distribution, the typical resistance increases as $\exp(L/\xi)$, and the mean resistance increases as $\exp(2L/\xi)$. This is in agreement with the universal scaling theory.[11,12,24]

As L exceeds L_ϕ, decoherence suppresses the resistance fluctuations and narrows the resistance distribution. As a result, at $L \gg L_\phi$ the mean resistance increases as $\beta L - c$ and the typical resistance as $\beta L - c'$, where β is the wire resistivity, c is a constant shift due to the decoherence near the source electrode, and $c' \gg c$ is the shift related to the resistance self-averaging in a single wire.

In the GaAs quantum wire the backscattering by disorder can be strong.[25] We therefore also examine the effect of strong disorder on coherent transport. We find deviations from universal scaling which differ from those reported for the Anderson model.[26]

In Sect. II we review the universal scaling theory and introduce our microscopic model of coherent 1D transport. In Sect. III the effect of strong disorder on coherent transport is discussed and deviations from universal scaling are reported. In Sect. IV we describe our decoherence model. Results of the decoherence model are presented in Sect. V. Discussion and conclusions are given in Sect. VI.

II. COHERENT 1D TRANSPORT

Electron transport in a disordered 1D wire with a single conducting channel is described in a simple way, if one assumes coherent transport of non-interacting quasiparticles. The wire resistance ρ (in units $h/2e^2$) reads[4,5,6]

$$\rho = \frac{R(\varepsilon_F)}{T(\varepsilon_F)}, \tag{1}$$

where R and T are the reflection and transmission coefficients describing the electron tunneling through disorder at Fermi energy. If disorder is specified by a random 1D potential $V(x)$, then R and T can be obtained as

$$R = |r_k|^2, \qquad T = |t_k|^2 \tag{2}$$

by solving the tunneling problem

$$\left[-\frac{\hbar^2}{2m}\,\frac{\mathrm{d}^2}{\mathrm{d}x^2} + V(x)\right]\Psi_k(x) = \mathcal{E}\Psi_k(x), \tag{3}$$

$$\Psi_k\,(x \to 0) = e^{ikx} + r_k e^{-ikx}, \tag{4}$$

$$\Psi_k\,(x \to L) = t_k e^{ikx}, \tag{5}$$

where $\Psi_k(x)$ is the 1D electron wave function, $\mathcal{E} = \hbar^2 k^2/2m$ is the electron energy, m is the effective mass, L is the wire length (the source contact is assumed at $x = 0$, the drain contact at $x = L$), and r_k and t_k are the reflection and transmission amplitudes.

The wire resistance (1) however depends on microscopic details of disorder and wildly fluctuates from wire

to wire in an ensemble of macroscopically identical wires. Therefore, instead of the resistance ρ of a single disordered wire the resistance distribution $p(\rho)$ is meaningful. For weak disorder $p(\rho)$ is given by the DMPK equation.[12] For a single-channel wire the DMPK equation reads[27]

$$\xi \frac{\partial}{\partial L} p(\rho, L) = \frac{\partial}{\partial \rho} \left[\left(\rho^2 + \rho\right) \frac{\partial}{\partial \rho} p(\rho, L) \right], \qquad (6)$$

where ξ is the electron localisation length. Now we review those properties of eq. 6, to which we refer later on.

From (6) one easy obtains the mean resistance

$$\bar{\rho}(L) \equiv \int_0^\infty d\rho \ \rho \ p(\rho, L) = \frac{1}{2} \left[\exp(2L/\xi) - 1\right], \qquad (7)$$

and also the mean square

$$\bar{\rho^2}(L) \equiv \int_0^\infty d\rho \ \rho^2 p(\rho, L) = \frac{1}{12} \left[2\exp(6L/\xi) - 6\exp(2L/\xi) + 4\right]. \qquad (8)$$

One sees that the dispersion $\left(\bar{\rho^2} - \bar{\rho}^2\right)^{1/2}/\bar{\rho} \simeq \exp(L/\xi)$ for $L/\xi \gg 1$, which means that $\bar{\rho}$ is not representative of the ensemble. Anderson et al.[11] proposed to average the variable $f = \ln(1+\rho)$. From eq. (6) one finds

$$\bar{f} \equiv \int_0^\infty d\rho \ln(1+\rho) p(\rho, L) = \frac{L}{\xi} \qquad (9)$$

and in a similar way (but in the limit $L/\xi \gg 1$) also

$$\Delta^2 \equiv \bar{f^2} - \bar{f}^2 = \frac{2L}{\xi}. \qquad (10)$$

Now the dispersion $\Delta/\bar{f} = (L/2\xi)^{-1/2}$ decreases with L/ξ, so $\bar{f}$ is representative of the ensemble. If one defines $p(\rho, L) = (1+\rho)^{-1}\mathcal{P}(\ln(1+\rho), L)$, eq. (6) readily gives

$$\mathcal{P}(\ln\rho, L) = \frac{1}{\sqrt{2\pi\Delta^2}} \exp\left[-\frac{\left(\ln\rho - \bar{f}\right)^2}{2\Delta^2}\right] \qquad (11)$$

for $\rho \gg 1$ (the case whenever $L/\xi \gg 1$). Expression (11) is a Gauss distribution centered at $\bar{f} = L/\xi$ with a spread $\Delta^2 = 2\bar{f} = 2L/\xi$. Thus, $p(\rho, L)$ is a log-normal distribution with a Gaussian-shaped bulk parametrized by $\bar{f} = L/\xi$. The moments of the distribution $p(\rho, L)$ [eqs. 7, 8] are dominated by the $1/\rho$ tail. One can introduce[11] the typical resistance ρ_t by definition $\ln(1+\rho_t) = \bar{f}$. For coherent transport

$$\rho_t(L) = \exp(L/\xi) - 1, \qquad (12)$$

since $\bar{f} = L/\xi$. Obviously, the distribution (11) is peaked at $\rho = \rho_t$, i.e., ρ_t is insensitive to the tail of $p(\rho, L)$.

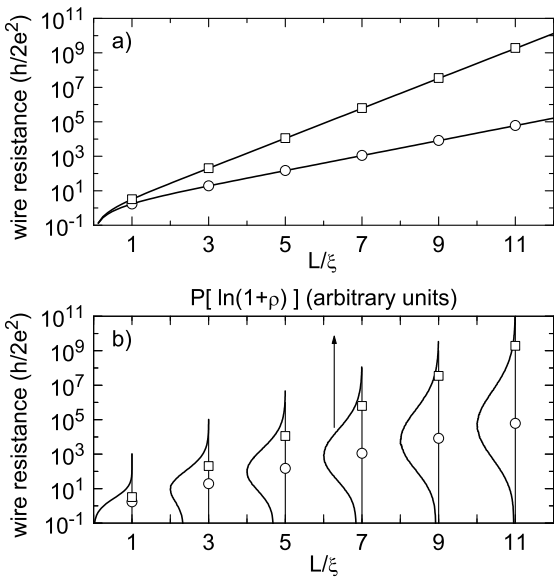

FIG. 1: (a) Mean resistance (squares) and typical resistance (circles) versus the scaling parameter L/ξ for the 1D wire with weak disorder as described in the text. Squares and circles are the microscopic model data, lines connecting these data are graphic representation of the formulae (7) and (12), respectively. (b) Distribution $\mathcal{P}(\ln(1+\rho))$ versus ρ: microscopic results for the same L/ξ as the squares and circles.

Equations (6)–(12) are macroscopic, their fundamental feature is the universal scaling with a single macroscopic parameter L/ξ. Now we describe our microscopic model.

We consider disorder $V(x) = \sum_{i=1}^N \gamma\delta(x - x_i)$, where $\gamma\delta(x - x_i)$ is the δ-shaped impurity potential of strength γ, x_i is the i-th impurity position (selected at random along the wire), and N is the number of impurities. We select N at random from the Poisson distribution

$$\mathcal{G}(N) = (N_I L)^N e^{-N_I L}/N! \qquad (13)$$

where N_I is the linear impurity density. The reflection coefficient of a single δ-barrier is $R_I = \Omega^2/(k_F^2 + \Omega^2)$, where $\Omega = m\gamma/\hbar^2$. We fix $k_F = 7.9 \times 10^7$ m^{-1} and $m = 0.067 m_0$, and we parameterize the δ-barrier by R_I.

We ignore the fluctuations of R_I, because they make the presentation less transparent but all major results remain the same (for weak disorder universal scaling holds independently on the choice of disorder) or similar (for strong disorder).

The scheme of the microscopic modeling is simple. We select disorder, solve eq. (3) by the transfer matrix method,[28] and obtain from eq. (1) the resistance of a single wire. We repeat this process for the ensemble of wires and obtain the resistance distribution and mean values.

Figure 1 shows results of the microscopic model for $R_I = 0.01$ and $N_I = 10^6$ m^{-1}. Since $R_I \ll 1$ and $N_I^{-1} \gg 2\pi/k_F$, we can speak about the weak low-density disorder. In such case eqs. (6-12) hold for[11,12]

$$\xi = l = (N_I R_I)^{-1}, \qquad (14)$$

where l is the classical elastic mean free path (100 μm in our case). If we set this value into eqs. (7) and (12), they indeed reproduce the microscopic data in Fig. 1a. We also see in Fig. 1b, that with increasing L/ξ the distribution $\mathcal{P}(\ln(1+\rho))$ tends to center around the typical resistance, while the mean resistance is essentially out of the distribution. This $\mathcal{P}(\ln(1+\rho))$ dependence can be reproduced by the formula (11) with $\xi = 100$ μm.

In summary, microscopic model and the scaling theory give the same results, as one expects for weak disorder. However, in the 1D GaAs wire the backscattering from a single impurity can be quite strong[25] ($R_I \approx 0.1 - 0.9$). In the next section we show that this can cause peculiar deviations from universal scaling.

III. DEVIATIONS FROM UNIVERSAL SCALING

We still consider the chain of N randomly-positioned identical δ-barriers at density as low as $N_I^{-1} \gg 2\pi/k_F$. For $N_I^{-1} \gg 2\pi/k_F$ useful exact expressions hold. The mean resistance reads

$$\bar{\rho}(N) = \frac{1}{2}\left[\left(\frac{1+R_I}{1-R_I}\right)^N - 1\right], \tag{15}$$

as shown for the first time by Landauer.[4] We rederive this expression in a more simple way in the Appendix. In the Appendix we also derive the mean square

$$\bar{\rho^2}(N) = \frac{1}{12}\left[2\left(1+\frac{6R_I}{(1-R_I)^2}\right)^N - 6\left(\frac{1+R_I}{1-R_I}\right)^N + 4\right] \tag{16}$$

and the typical resistance

$$\rho_t(N) = \left(\frac{1}{1-R_I}\right)^N - 1. \tag{17}$$

Equations (15–17) are exact for any R_I, if $N_I^{-1} \gg 2\pi/k_F$. Averaging them over the distribution (13) we include fluctuations of N. We obtain equations

$$\bar{\rho}(L) = \frac{1}{2}\left[\exp\left(2N_I\frac{R_I}{1-R_I}L\right) - 1\right], \tag{18}$$

$$\bar{\rho^2}(L) = \frac{1}{12}\left[2\exp\left(6N_I\frac{R_I}{(1-R_I)^2}L\right) - 6\exp\left(2N_I\frac{R_I}{1-R_I}L\right) + 4\right], \tag{19}$$

$$\rho_t(L) = \exp\left[N_I\ln\left(\frac{1}{1-R_I}\right)L\right] - 1, \tag{20}$$

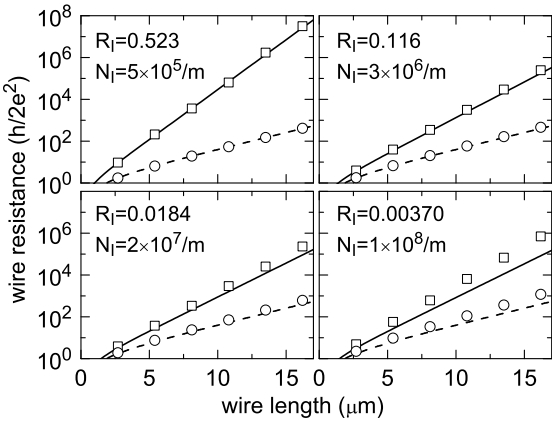

FIG. 2: Mean resistance (squares, full lines) and typical resistance (circles, dashed lines) versus the wire length L. Squares and circles are the microscopic model results, full lines and dashed lines are graphic representation of the formulae (18) and (20), respectively. Parameters N_I and R_I are varied in such way that the localization length (21) is the same ($\xi = 2.7$ μm) for each figure. One can see that the accuracy of eqs. (18) and (20) deteriorates with increasing N_I.

which provide us with the exact dependence on L.

Let us compare eqs. (18), (19), and (20) with the scaling theory equations. Comparing eq. (20) with eq. (12) we get the localisation length

$$\xi = \left[N_I\ln\left(\frac{1}{1-R_I}\right)\right]^{-1}. \tag{21}$$

Comparing eq. (18) with eq. (7) we obtain the length

$$\xi_1 = \left(N_I\frac{R_I}{1-R_I}\right)^{-1}, \tag{22}$$

where index 1 is added to distinguish from ξ. Finally, comparing eq. (19) with eq. (8) we again find the length (22) and additionally the length

$$\xi_2 = \left[N_I\frac{R_I}{(1-R_I)^2}\right]^{-1}. \tag{23}$$

A comment on the accuracy of the above equations. If $N_I^{-1} \gg 2\pi/k_F$, our microscopic model gives results, which agree with eqs. (18)–(20) for any value of R_I. Otherwise, a simple phase averaging used in the Appendix [eqs. (A2), (A7), (A11)] is no longer accurate and the accuracy of eqs. (18)–(20) deteriorates as we demonstrate in Fig. 2. In such case eqs. (21)–(23) are not reliable as well and we have to obtain ξ, ξ_1, and ξ_2 directly from the microscopic model. (This means that we fit the microscopic model results by the formulae (12), (7), and (8) with a properly adjusted ξ, ξ_1, and ξ_2, respectively. To obtain the localization length ξ, we can also use the Lyapunov exponent analysis,[29] but we get the same result.) In this section we restrict us to the limit

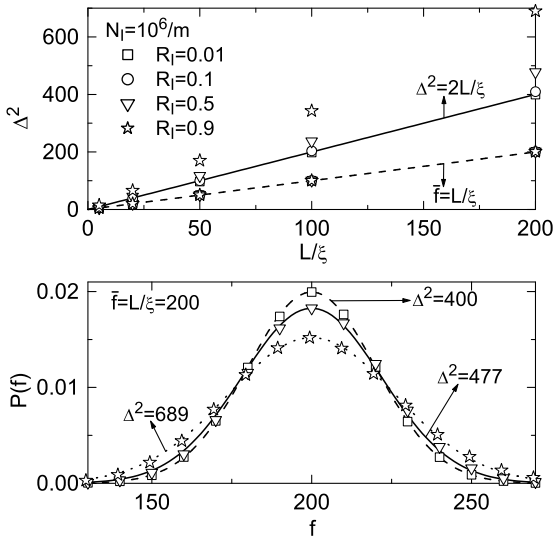

FIG. 3: The top figure: Mean deviation $\Delta^2 \equiv \bar{f^2} - \bar{f}^2$ versus L/ξ (ξ is given by eq. (21)) for various R_I. The microscopic model (symbols) is compared with the scaling theory result $\Delta^2 = 2L/\xi$ (full line). Also is compared $\bar{f} = L/\xi$ (dashed line) with $\bar{f}$ obtained from the microscopic model (symbols coinciding with the dashed line). The bottom figure: Distribution $\mathcal{P}(f)$ for $L/\xi = 200$. Symbols show the microscopic results for various R_I. Lines connecting points are the Gauss distributions (11) with Δ^2 as indicated, the indicated data are microscopic data from the top figure.

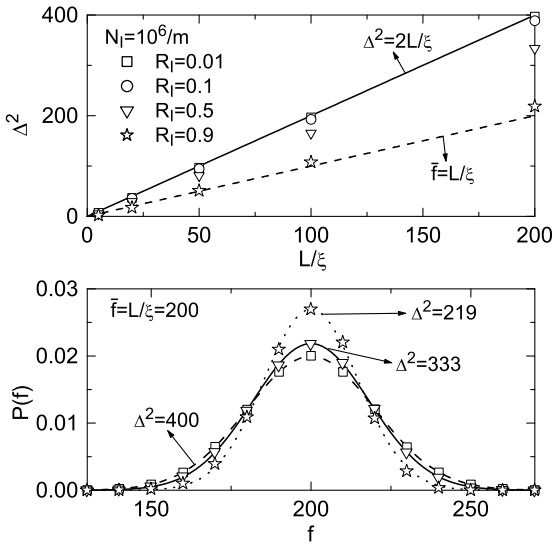

FIG. 4: The same calculation as in Fig. 3, but with N fixed to its mean value $N_I L$. Also symbols have the same meaning as in Fig. 3.

$N_I^{-1} \gg 2\pi/k_F$, because eqs. (18), (19), and (20) are useful and our conclusions would remain similar also beyond the limit $N_I^{-1} \gg 2\pi/k_F$.

Equations (18), (19), and (20) scale with three parameters L/ξ, L/ξ_1, and L/ξ_2 and coincide with eqs. (7), (8), and (12) only in the limit $R_I \ll 1$, when $\xi = \xi_1 = \xi_2 = (N_I R_I)^{-1}$. Since the moments (18) and (19) do not scale with the same parameter as the typical resistance (20), this invokes that also the bulk of the distribution, i.e., $\mathcal{P}(\ln(1+\rho))$, does not scale with a single parameter.

Our microscopic model indeed shows that the distribution $\mathcal{P}(\ln(1+\rho))$ scales with two parameters. This is demonstrated in Fig. 3 for various R_I and for $N_I = 10^6$ m^{-1}. The top figure shows that for large R_I the mean deviation Δ^2 does not scale as $2L/\xi$. It can be seen that in general $\Delta^2 > 2L/\xi$. Further, as shown in the bottom figure, the microscopically calculated $\mathcal{P}(\ln(1+\rho))$ coincides with the Gauss distribution (11) centered at $\bar{f} = L/\xi$, but its spread Δ^2 is no longer $2L/\xi$.

Two-parametric scaling has already been reported for the 1D Anderson model,[26] in which disorder is due to the equidistant barriers with a barrier strength fluctuating at random. It has been found[26] that $\Delta^2 < 2L/\xi$ rather than $\Delta^2 > 2L/\xi$. This difference is due to the fact that in our model N fluctuates from wire to wire, as is the case for impurity disorder in real samples. If we fix N in each wire to its mean value $N_I L$, we also obtain $\Delta^2 < 2L/\xi$ (see Fig. 4). The two-parameter scaling (Fig. 4) is then similar to that one in the Anderson model.[26]

Why the fluctuating N enhances Δ^2 in comparison with the case $N = N_I L$? In the ensemble with fluctuating N the wires with $N > N_I L$ ($N < N_I L$) typically contribute into the resistance distribution by larger (smaller) resistance values than the wires with $N = N_I L$. This broadens the distribution.

Why the fluctuating N does not affect Δ^2 in the limit of small R_I? The dispersion of N is $1/\sqrt{N_I L}$. As R_I approaches zero, L approaches infinity in order to keep a constant L/ξ. The dispersion of N thus becomes negligible, so one obtains $\Delta^2 = 2L/\xi$ for the fluctuating as well as fixed N (c.f. Figs. 3 and 4).

IV. DECOHERENCE MODEL

Now we assume that the electron motion along the wire is perturbed by inelastic collisions. An electron will move coherently with a certain energy for a while, suffer an inelastic collision which will transfer it to another energy, move coherently with the new energy, suffer another inelastic collision and so on. Thus, electron motion across disorder is no longer elastic and the final states after inelastic collisions are in general affected by the blocking effect of Pauli principle. In this situation the applicability of the Landauer expression (1) is questionable.

However, as pointed out in Ref. 6, expression (1) is still applicable if one assumes that there is no net "vertical" flow of electrons: every electron that scatters out of its energy $\mathcal{E}_1$ into another energy $\mathcal{E}_2$ is balanced by another electron that scatters out of $\mathcal{E}_2$ into $\mathcal{E}_1$. This effectively means that an electron with a given energy moves coherently for a while, suffers a phase-breaking

collision, continues to move coherently with the same energy, suffers another phase-breaking collision and so on. This "effective" electron feels the phase-breaking collisions like elastic events and the effect of Pauli blocking disappears. Transport thus still proceeds via independent energy channels and can be described in terms of the transmission and reflection as does equation (1). However, the transmission of electrons from one contact to the other is now characterised by repeated phase breaking rather than by a single coherent process.

To account for the repeated phase breaking in a simple way we further assume that each phase-breaking collision randomizes the electron phase completely.[30] In such case it is expected[31] and can be shown rigorously,[18] that the phase-breaking events break the wire into segments where each segment is an independent series resistor with coherent electronic resistance. The resistance of each segment can thus be evaluated from the Landauer resistance formula and the resistance of the wire is simply a sum of the resistances of all segments.

We recall that our model relies on the assumption that there is no net "vertical" flow. This assumption is exact for the e-e interaction. Indeed, if only the e-e interaction is operative, then there is no energy exchange between the electrons and crystal lattice, so any non-zero "vertical" flow would distort the electron energy distribution. In fact the e-e interaction maintains a thermalised distribution,[23] i.e., there is no such distortion. Moreover, the e-e interaction conserves the total momentum of the 1D gas and does not cause any momentum-relaxation related resistance. All these features are inherent to our model, so we believe that we have a reasonable phenomenological model of the e-e interaction mediated phase breaking.

Now we give details of our model. Consider a single wire with specified disorder. Assume that an electron at the Fermi level undergoes N inelastic collisions when traversing the wire length L. Denote the time elapsed between the $n-1$ and n collisions as $\tau_{n-1,n}$ and the positions of these collisions along the wire as x_{n-1} and x_n. Due to disorder the electron motion is diffusive, therefore

$$(x_n - x_{n-1})^2 = D\tau_{n-1,n}, \tag{24}$$

where D is the elastic diffusion coefficient. The wire is divided into segments $x_n - x_{n-1}$, where each segment is a series resistor with coherent resistance $\rho(x_n - x_{n-1})$. We evaluate $\rho(x_n - x_{n-1})$ from eq. (1) by solving eq. (3) for the boundary conditions (4) and (5) applied at the boundaries x_{n-1} and x_n. The resistance of the segmented wire reads $\rho(\tau_{0,1}) + \rho(\tau_{1,2}) + \cdots + \rho(\tau_{N-1,N}) + \rho(\tau_{N,L})$, where the variable $\tau_{n-1,n}$ is used instead of $x_n - x_{n-1}$ and the positions at the beginning and end of the wire are denoted as 0 and L.

Of course, when transmitted from the source to the drain, each Fermi electron experiences a different random configuration of segments. Therefore, the resistance of the segmented wire has to be averaged over all possible configurations of segments, taken with a proper weight.

For this purpose, denote the inelastic scattering rate as $1/\tau_{in}$. Let $P(\tau)$ be the probability that the electron moves without inelastic collision for time τ. The probability that one inelastic collision occurs in time $(\tau, \tau+d\tau)$ is given by $P(\tau)d\tau/\tau_{\rm in} = P(\tau) - P(\tau + d\tau)$, which gives

$$P(\tau)\frac{d\tau}{\tau_{\rm in}} = \exp\left(-\frac{\tau}{\tau_{\rm in}}\right)\frac{d\tau}{\tau_{\rm in}}. \tag{25}$$

For $N = 0$ the weighted resistance is simply

$$\rho_{N=0}(L) = \rho(\tau_{0,L})\exp\left(-\frac{\tau_{0,L}}{\tau_{\rm in}}\right), \tag{26}$$

where $\tau_{0,L} = L^2/D$ is the elastic diffusion time from the source up to the drain. Similarly, for $N = 1$ one finds

$$\rho_1(L) = \int_0^{\tau_{0,L}} \frac{d\tau_{0,1}}{\tau_{\rm in}} \exp\left(-\frac{\tau_{0,1}}{\tau_{\rm in}}\right)\exp\left(-\frac{\tau_{1,L}}{\tau_{\rm in}}\right) \times \left[\rho(\tau_{0,1}) + \rho(\tau_{1,L})\right], \tag{27}$$

where $L = \sqrt{D}\left(\sqrt{\tau_{0,1}} + \sqrt{\tau_{1,L}}\right)$, because the segments must add to give the total wire length L. Analogously,

$$\rho_2(L) = \int_0^{\tau_{0,L}} \frac{d\tau_{0,1}}{\tau_{\rm in}} \int_0^{\tau_{1,2}^{\max}} \frac{d\tau_{1,2}}{\tau_{\rm in}} \times \exp\left(-\frac{\tau_{0,1}}{\tau_{\rm in}}\right)\exp\left(-\frac{\tau_{1,2}}{\tau_{\rm in}}\right)\exp\left(-\frac{\tau_{2,L}}{\tau_{\rm in}}\right) \times \left[\rho(\tau_{0,1}) + \rho(\tau_{1,2}) + \rho(\tau_{2,L})\right], \tag{28}$$

where $L = \sqrt{D}\left(\sqrt{\tau_{0,1}} + \sqrt{\tau_{1,2}} + \sqrt{\tau_{2,L}}\right)$ and $\tau_{1,2}^{\max} = \left(\sqrt{\tau_{0,L}} - \sqrt{\tau_{0,1}}\right)^2$. It is easy to generalize $\rho_2(L)$ to $\rho_N(L)$ and to express the averaged resistance as

$$\rho(L) = \sum_{N=0}^{\infty}\rho_N(L) = \sum_{N=0}^{\infty}\int_0^{\tau_{0,L}}\frac{d\tau_{0,1}}{\tau_{\rm in}}\int_0^{\tau_{1,2}^{\max}}\frac{d\tau_{1,2}}{\tau_{\rm in}}\cdots \times \int_0^{\tau_{N-1,N}^{\max}}\frac{d\tau_{N-1,N}}{\tau_{\rm in}}\exp\left(-\frac{\tau_{0,1}}{\tau_{\rm in}}\right)\exp\left(-\frac{\tau_{1,2}}{\tau_{\rm in}}\right)\cdots \times \exp\left(-\frac{\tau_{N-1,N}}{\tau_{\rm in}}\right)\exp\left(-\frac{\tau_{N,L}}{\tau_{\rm in}}\right) \times \left[\rho(\tau_{0,1}) + \rho(\tau_{1,2}) + \cdots + \rho(\tau_{N-1,N}) + \rho(\tau_{N,L})\right], \tag{29}$$

where $L/\sqrt{D} = \sqrt{\tau_{0,1}} + \sqrt{\tau_{1,2}} + \cdots + \sqrt{\tau_{N-1,N}} + \sqrt{\tau_{N,L}}$ and $\tau_{n-1,n}^{\max} = \left(\sqrt{\tau_{0,L}} - \sqrt{\tau_{0,1}} - \sqrt{\tau_{1,2}} - \cdots - \sqrt{\tau_{n-2,n-1}}\right)^2$.

We recall that eq. (29) gives the resistance of a wire with specific configuration of disorder. Evaluating eq. (29) for the ensemble of wires with different configurations of disorder we can obtain numerically the resistance distribution and the mean and typical resistance.

One has to be careful when evaluating the typical resistance. Our derivation of eq. (29) is motivated by Ref. 32, which uses similar considerations to derive the typical resistance. Equation (3.7) in Ref. 32 should coincide with our result (29), but it does not: the limits $\tau_{n-1,n}^{\max}$ are different. Another problem, physical rather than technical, is the following. It is tempting to follow Ref. 32 and to set for each segment in eq. (29) the typical coherent resistance

$$\rho(\tau_{n-1,n}) = \exp\left(\frac{\sqrt{D\,\tau_{n-1,n}}}{\xi}\right) - 1. \qquad (30)$$

However, the typical resistance of the segmented wire is not a sum of typical resistances of the individual segments. A correct approach is to obtain the ensemble average $\bar{f}$ of the quantity $f = \ln(1+\rho(L))$, where $\rho(L)$ is given by eq. (29), and to extract the typical resistance from definition $\ln(1+\rho_t) = \bar{f}$.

On the other hand, the mean resistance of the segmented wire as a direct ensemble average of eq. (29) is a sum of mean resistances of individual segments. Thus, if we set for each segment the mean coherent resistance

$$\rho(\tau_{n-1,n}) = \frac{1}{2}\left[\exp\left(\frac{2\sqrt{D\,\tau_{n-1,n}}}{\xi_1}\right) - 1\right], \qquad (31)$$

then eq. (29) expresses the mean resistance of the wire.

We have derived eq. (29) to provide insight and to give a formal expression for the wire resistance. Now we describe another averaging procedure, a Monte Carlo approach, which does not provide any formulae, but is much easier to implement and gives the same numerical results.

We start by specifying disorder in a given wire. The segmentation of the wire is then simulated as a Monte Carlo process, in which the time τ between two inelastic collisions is selected at random from equation

$$r = \int_0^{\tau} \frac{d\tau}{\tau_{\rm in}} \exp\left(-\frac{\tau}{\tau_{\rm in}}\right) = 1 - \exp\left(-\frac{\tau}{\tau_{\rm in}}\right), \qquad (32)$$

where r is a random number between 0 and 1. We generate the times $\tau_{0,1}$, $\tau_{1,2}$, $\tau_{2,3}, \ldots$. After each time generation we determine the total segmented length, say $\sqrt{D\tau_{0,1}} + \sqrt{D\tau_{1,2}} + \sqrt{D\tau_{2,3}}$, and we check whether it does not exceed L. If it does not, we generate $\tau_{3,4}$. If it does, we obtain the length of the rest, $\sqrt{D\tau_{2,L}} = L - \left(\sqrt{D\tau_{0,1}} + \sqrt{D\tau_{1,2}}\right)$. Thus, the position and length of each segment between the source and drain are known. We evaluate the coherent resistance of each segment and sum the resistances of all segments to obtain the total resistance of the segmented wire. We repeat this segmentation process for the same wire many times and average the wire resistance over all configurations of segments (numerical results are the same as gives eq. (29)). We apply the described procedure to the ensemble of wires with various configurations of disorder and obtain the resistance distribution and ensemble-averaged quantities.

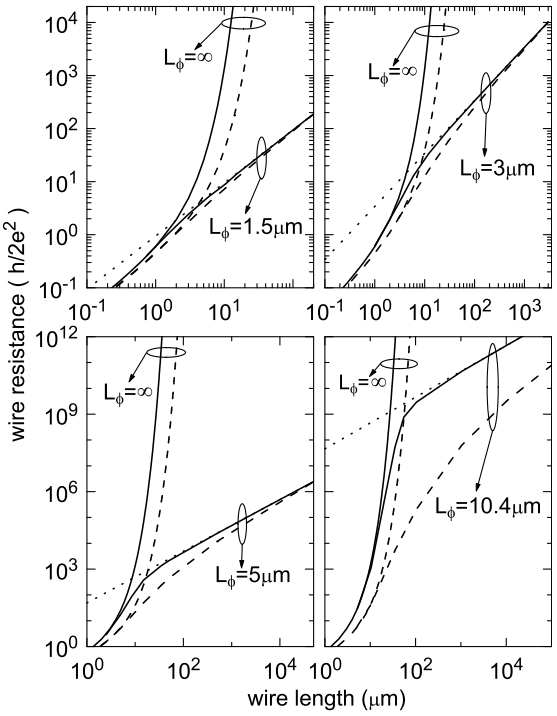

FIG. 5: The mean resistance (solid lines) and typical resistance (dashed lines) of the 1D wire as functions of the wire length L for various coherence lengths L_ϕ. The coherent resistance ($L_\phi = \infty$) is shown for comparison. The dotted line shows the linear βL slope (see the text) to which the mean and typical resistances converge at large L. In these calculations disorder with parameters $N_I = 3\times10^6$ m^{-1} and $R_I = 0.116$ was used, for these parameters the microscopic approach of Sect. III gives $\xi = 2.65$ μm, $\xi_1 = 2.47$ μm, and $\xi_2 = 2.15$ μm.

A comment about the parameters of our decoherence model. Coefficient D describes coherent diffusion across disorder. Since the coherent resistance fluctuates from segment to segment, also D should be evaluated for each segment separately. For simplicity, we assume in each segment the same D. This allows us to substitute the variable τ by the variable $s = \sqrt{D\tau}$ in all formulae of this section and we get rid of D. The only parameter is thus τ_{in}. Since the electron coherence length is $L_\phi = \sqrt{D\tau_{in}}$, in what follows we refer to L_ϕ rather then to τ_{in}.

At low enough temperatures the electron-phonon interaction is suppressed, which we assume. In such case L_ϕ is governed by e-e interactions and the calculation of L_ϕ for a disordered single-moded 1D wire is a formidable task. We therefore consider L_ϕ as a parameter.

V. RESULTS OF DECOHERENCE MODEL

In Fig. 5 we show the mean and typical resistances in presence of decoherence for various values of L_ϕ and for disorder as specified in the figure caption. Disorder gives the localization length $\xi = 2.65$ μm, roughly this value is typical say for a V-groove GaAs quantum wire.[33] We

vary L_ϕ from smaller to larger values than ξ, since at low temperatures crossover of this kind is expected.

Figure 5 also shows the mean and typical resistance in the coherent regime ($L_\phi = \infty$). For $L < L_\phi$ the resistance with decoherence and the coherent resistance coincide as one expects. For $L > L_\phi$ both the mean and typical resistance are driven by decoherence towards a linear dependence on L. The slope of this linear dependence is shown in a dotted line, note that the mean resistance reaches the linear slope at much smaller L than does the typical resistance. Now we discuss these results in detail.

A. Resistivity and mean resistance

The slope of the linear dependence in Fig. 5 gives the wire resistivity, β. For an infinite wire we expect

$$\beta = \frac{\int_0^\infty ds\, g(s)\, \rho(s)}{\int_0^\infty ds\, g(s)\, s}, \tag{33}$$

where $\rho(s) = 0.5\,[\exp(2s/\xi_1) - 1]$, s is the length of the segment, and the s–distribution for the (infinite) wire is

$$g(s) = \frac{2s}{L_\phi^2}\, e^{-\frac{s^2}{L_\phi^2}}, \tag{34}$$

as follows from eq. (25) for $s = \sqrt{D\tau}$. Equation (33) gives[34]

$$\beta = \frac{1}{\xi_1}\, \exp\left(\frac{L_\phi^2}{\xi_1^2}\right)\left[1 + \mathrm{erf}\left(\frac{L_\phi}{\xi_1}\right)\right] \tag{35}$$

and the dotted line in Fig. 5 shows the dependence βL. Clearly, the slope of the dotted line coincides with the linear slope to which the decoherence drives the mean and typical resistance. Thus, eq. (35) correctly expresses the wire resistivity. We have not attempted to do so, but eq. (35) should be derivable directly from eq. (29).

The log-scale in Fig. 5 obscures an interesting effect. In Fig. 6 we present the mean resistance from Fig. 5 in a linear scale. Clearly, the ohmic dependence to which the decoherence drives the mean resistance is not βL, but $\beta L - c$, where $c > 0$ is a constant shift. The shift increases with L_ϕ and diminishes for $L_\phi = 0$, it should be observed in the 1D wires long enough to exhibit the ohmic resistance. As discussed below, this shift is a "memory effect" reflecting the decoherence near the source contact.

To give insight we approximate the exact mean resistance (the ensemble-averaged equation (29)) as

$$\bar{\rho}(L) \approx \frac{1}{2}\,(e^{\frac{2L}{\xi_1}} - 1)\, e^{-\frac{L^2}{L_\phi^2}} + (1 - e^{-\frac{L^2}{L_\phi^2}}) \int_0^L dx \beta(x), \tag{36}$$

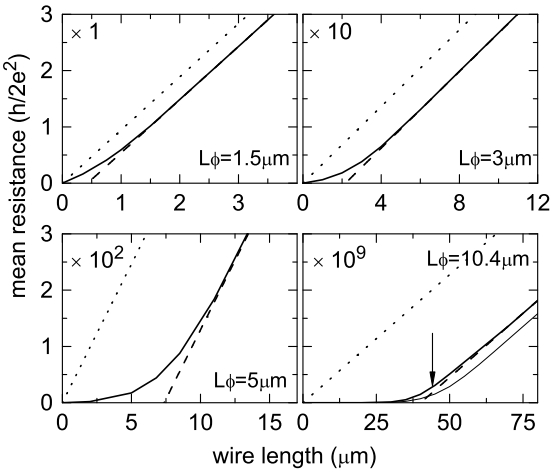

FIG. 6: The mean resistance from Fig. 5 shown in a linear scale: the dotted line shows the dependence βL, the full line is the mean resistance resulting from the decoherence model, the dashed line is the shifted βL dependence to which the mean resistance actually converges. The resistance data should be multiplied by a factor 1, 10, 10^2, or 10^9, as indicated. The arrow and thin full line are discussed in the text.

where x is the distance from the source electrode and

$$\beta(x) = \frac{\int_0^x ds\, g(s)\, \frac{1}{2}\,(e^{\frac{2s}{\xi_1}} - 1)}{\int_0^x ds\, s\, g(s)} \tag{37}$$

is the resistivity (33) approximated for a finite wire. The first term on the right hand side of eq. (36) coincides with the first term of the ensemble-averaged sum (29) and the term $\int_0^L dx\beta(x)$ approximates the rest of the sum (see below). The first term is the contribution from coherent transmission while the term $\int_0^L dx\beta(x)$ describes the contribution from incoherent transmission. The weight $1 - \exp(-L^2/L_\phi^2)$ is the probability that the transmission is not coherent, it tailors both terms at $L \approx L_\phi$.

Equation (37) accounts for the fact that decoherence in the wire increment $(0, x)$ does not involve segments larger than x, but it still relies on eq. (34), which strictly holds only for the infinite wire.[35] The question is now how good is eq. (36). In Fig. 6 the dependence (36) is shown in the thin full line for $L_\phi = 10.4$ μm. It reasonably fits the thick full line, with increasing L_ϕ/ξ_1 (not shown) the fit is even better.

Equation (36) thus explains the shift c in the limit $L_\phi \gg \xi_1$. It that limit $\beta(x) \ll \beta$ for x smaller than a certain distance L_0, while for $x > L_0$ $\beta(x) \simeq \beta$. Indeed, the function $g(s)\,\rho(s)$ is peaked at

$$L_0 \equiv \frac{L_\phi^2}{\xi_1} \tag{38}$$

and then steeply decreases to zero, so that $\beta(x) \simeq \beta$ for $x > L_0$. Similarly the coherent term in eq. (36) reaches

maximum at $L = L_0$ and then steeply decreases to zero. Therefore, $\bar{\rho}(L) \simeq \beta L - c$ for $L > L_0$, in accord with Fig. 6, where L_0 is labeled by an arrow.

In other words, after leaving the source the Fermi electron first overcomes the distance L_0 at which it acquires the mean resistance $\bar{\rho}(L_0) \ll \beta L_0$. Beyond this distance it contributes ohmically but the shift $c \approx \beta L_0$ is fixed.

Figure 6 suggests that L_ϕ and ξ_1 might in principle be measurable as follows. Measuring the mean resistance in the linear regime (in long wires) one could determine β. One could then extrapolate this linear dependence up to the intersection point with the L-axis, determine L_0 as the L-value at the intersection point, and obtain L_ϕ and ξ_1 from eqs. (35) and (38). This is justified if $L_\phi/\xi_1 \gg 1$, i.e., if the intersection point and L_0 coincide (in Fig. 6 these points are still slightly separated for $L_\phi = 10.4$ μm). One could also directly measure ξ_1 (by detecting the $0.5\,[\exp(2L/\xi_1) - 1]$ dependence in wires shorter than L_ϕ) and obtain L_ϕ from eq. (35). All this is however difficult in practice, as we discuss below.

B. Is the mean resistance measurable in practice?

To address this question we need to calculate the resistance dispersion $d(L) \equiv (\bar{\rho^2}(L) - \bar{\rho}^2(L))^{1/2}/\bar{\rho}(L)$. In the coherent regime we insert for $\bar{\rho}(L)$ and $\bar{\rho^2}(L)$ the formulae (18) and (19), and we obtain the coherent dispersion

$$d_{coh}(L) = \sqrt{\frac{1}{3}\left[A-1\right]^{-2}\left[2B-6A+4\right]-1}, \qquad (39)$$

where $A = \exp(2L/\xi_1)$ and $B = \exp(6L/\xi_2)$. In Fig. 7 the coherent dispersion (39) is shown in a dashed line. It increases for large L even faster than its weak-disorder limit $\exp(L/\xi)$ since our disorder is not weak enough (note in the caption of Fig. 5 that $\xi_2 < \xi_1 < \xi$).

However, this fast increase diminishes in presence of decoherence. The full circles in Fig. 7 show the dispersion obtained from our decoherence model. It coincides with the coherent dispersion when $L < L_\phi$, but as L exceeds L_ϕ it tends to decrease like $L^{-1/2}$ rather than to increase. This is easy to understand. Consider an "incoherent wire" consisting of n independent coherent segments of length s. The resistance dispersion of each segment is given by eq. (39) as $d_{coh}(s)$ and the resistance dispersion of such wire is simply $d_{incoh} = n^{-1/2} d_{coh}(s) = (s/L)^{1/2} d_{coh}(s)$, i.e., $d_{incoh}(L) \propto L^{-1/2}$.

It seems reasonable to improve this simple model as

$$d_{incoh}(L) = \sqrt{\frac{\bar{s}}{L}} \int_0^L ds\, g(s)\, d_{coh}(s), \qquad (40)$$

where $g(s)$ is given by eq. (34) and $\bar{s} = \int_0^\infty ds\, g(s)\, s$, and to express the resistance dispersion of the wire as

$$d(L) = e^{-\frac{L^2}{L_\phi^2}}\, d_{coh}(L) + (1 - e^{-\frac{L^2}{L_\phi^2}})\, d_{incoh}(L), \qquad (41)$$

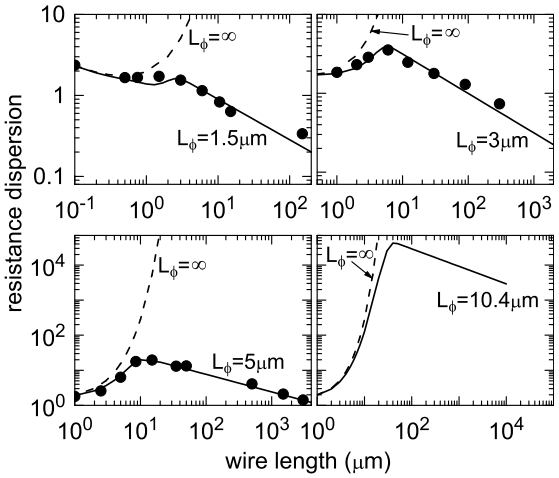

FIG. 7: Resistance dispersion versus the wire length L for the same parameters as Fig. 5. The dashed line shows the coherent result (39), dispersion with decoherence are the full circles (decoherence model of Sect. IV) and full lines [eq. (41)].

where $\exp(-L^2/L_\phi^2)$ is the coherent transmission probability. In Fig. 7 the dependence (41) is shown in the full line, its agreement with our decoherence model results is good. The decoherence model needs a lot of computational time to give the resistance dispersion with a reasonable accuracy and this time increases very fast with increasing L_ϕ/ξ_1. Therefore, in Fig. 7 no full circles are shown for $L_\phi = 10.4$ μm, but we believe that eq. (41) gives a reasonable information also in this case.

To measure $\bar{\rho}(L)$ in practice, one needs to measure the resistance of the ensemble of wires, of course, each wire in the ensemble has to be biased separately. Ideally, the wires should be identical as to their geometry, doping level, electron density, etc., and the number of the occupied 1D channels should be tunable up to the ground energy subband. Finally, the distance between the nearest wires should be say a few microns to exclude the electron-electron inter-wire coupling. All together, these conditions are difficult to realize in practice, but experiments with the ensembles of several tens to several hundreds of such wires might perhaps be realizable.

How many wires are needed to obtain a reliable ensemble average? Assume[36] that $\bar{\rho}(L)$ is measured with the error $d(L)/\sqrt{n_w}$, where n_w is the number of wires in the ensemble. To achieve for instance $d(L)/\sqrt{n_w} \approx 1/2$, in case of Fig. 7 we need $n_w \simeq 1 - 500$ for $L_\phi = 1.5 - 5$ μm while for $L_\phi = 10.4$ μm the upper limit of n_w as large as 10^{10} is needed. Generally speaking, $n_w \simeq 1 - 500$ suffices if $L_\phi/\xi_1 < 2$, for larger L_ϕ/ξ_1 the upper limit of n_w is simply too large to be realizable in practice. In the latter case $\bar{\rho}(L)$ is still measurable say for $d(L) < 10$, i.e., in the very short or very long wires.

To measure the resistance of millions of disordered wires it would be desirable to fabricate a single quantum wire with tunable disorder. We have in mind the wire in which intrinsic disorder is negligible but a tun-

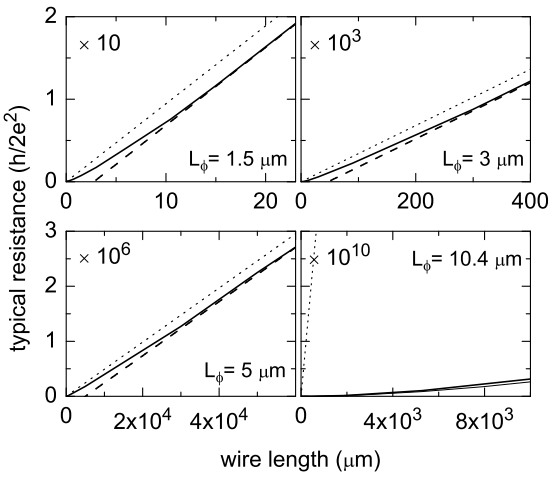

FIG. 8: The typical resistance from Fig. 5 shown in a linear scale: the dotted line shows the dependence βL, the full line is the typical resistance resulting from the decoherence model of Sect. IV, the dashed line is the shifted βL dependence to which the typical resistance converges. The resistance data should be multiplied by a factor 1, 10^3, 10^6, or 10^{10}, as indicated. The thin full line is the approximation of the typical resistance described by eqs. (42-48).

able extrinsic disorder is introduced by using an array of very narrow equidistant gates biased separately by a voltage varying at random from gate to gate. Biasing a single gate creates a localized potential barrier inside the wire underneath the gate. Thus, the array of the gates of width $\sim 2\pi/k_F$ would create disorder of equidistant random barriers, each of them with the quantum-reflection coefficient R_I tunable between 0 and 1 by external bias.

Perhaps a proper candidate for realization of tunable disorder is the cleaved-edge overgrowth quantum wire system, which shows ballistic transport (negligible intrinsic disorder) for wires as long as several tens of microns.[37] One could speculate about an array of gates, or instead of the gate array one could think about an array of separately biased non-invasive probes. Such probes were already realized in the cleaved-edge overgrowth wire[38] in a different context, they allow to tune also the wire length.

C. Typical resistance and distribution of $\ln(1+\rho)$

The typical resistance is defined as $\rho_t = \exp(\bar{f}) - 1$, where $\bar{f}$ is the ensemble average of the variable $f = \ln(1+\rho)$. Obviously, $\rho_t = \bar{\rho}$ if $\rho = \bar{\rho}$, i.e., if there are no resistance fluctuations. Since the resistance fluctuations decrease in presence of decoherence as $1/\sqrt{L}$ (c.f. Fig. 7), one might expect the typical resistance to approach the mean resistance with increasing L. Reality is however more complicated. We have seen in Fig. 5 that decoherence drives the typical resistance towards the same linear slope as it drives the mean resistance. In Fig. 8 we present the typical resistance again, but in a linear scale. Clearly, decoherence drives the typical resistance towards the linear dependence $\beta L - c'$, where the shift c' strongly differs from the shift c of the mean resistance (c.f. Fig. 6). The lines $\rho_t(L) \propto L$ and $\bar{\rho}(L) \propto L$ remain parallel, i.e., ρ_t differs from $\bar{\rho}$ also in the ohmic regime.

To give insight we wish to assess $\rho_t(L)$ more transparently. In analogy with eqs. (36) and (37), we approximate

$$\rho_t(L) \approx \rho(L)\, e^{-\frac{L^2}{L_\phi^2}} + (1 - e^{-\frac{L^2}{L_\phi^2}}) \int_0^L dx \beta_t(x), \qquad (42)$$

$$\beta_t(x) = \frac{\int_0^x ds\, g\,(s)\, \rho(s)}{\int_0^x ds\, s\, g\,(s)}, \qquad (43)$$

but we assess $\rho(s)$ as a typical resistance of the segment.

Imagine a segment s positioned in the beginning of a wire with specific disorder. If we move the segment along the wire, $\rho(s)$ fluctuates discretely each time an impurity leaves or enters the segment. However, since a single impurity scatters weakly, differences between the successive discrete values can be neglected except for resonant changes occurring (on average) whenever the segment is shifted by ξ. The number of such changes,

$$n = \mathrm{Int}\left[\frac{x-s}{\xi}\right] + 1, \qquad (44)$$

results in a serie of n different values of $\rho(s)$. Denoting this serie as $\rho_1(s)$, $\rho_2(s)$, ..., $\rho_n(s)$ we can write

$$\rho(s) = \frac{1}{n}\sum_{i=1}^{n} \rho_i(s) = \frac{1}{n}\sum_{i=1}^{n} (e^{f_i} - 1), \qquad (45)$$

where the variable $f_i = \ln(1+\rho_i(s))$ follows the coherent distribution $\mathcal{P}(f,s)$ discussed in Sects. II–III. Each f in a specific serie $f_1(s)$, $f_2(s)$, ... $f_n(s)$ can thus be viewed as a random number from that distribution. The so-called typical serie f_1, f_2, ..., f_n is given by equations

$$\frac{1}{n+1} = \int_0^{f_1} df \mathcal{P}(f) = \int_{f_1}^{f_2} df \mathcal{P}(f) = \cdots = \int_{f_{n-1}}^{f_n} df \mathcal{P}(f), \qquad (46)$$

because one expects that the total area $\int_0^\infty df\mathcal{P}(f) = 1$ is on average divided into $n+1$ areas of size $1/(n+1)$ (the argument s is skipped for simplicity). Using

$$\mathcal{P}(f) = \frac{1}{\sqrt{2\pi\Delta^2}} \exp\left[-\frac{(f-\bar{f})^2}{2\Delta^2}\right], \qquad \bar{f} = s/\xi \qquad (47)$$

we get from eq. (46) the equations

$$\mathrm{erf}\left(\frac{f_i - \bar{f}}{\sqrt{2\Delta^2}}\right) = \frac{2i}{n+1} - 1, \qquad i = 1, \ldots, n. \qquad (48)$$

Equation (47) is an approximation valid for $s/\xi \gg 1$. It roughly holds for any s/ξ, if one adjusts[11] Δ^2 to fulfill the equation $\int df\mathcal{P}(f)(\exp(f)-1) = 0.5\,[\exp(2s/\xi_1)-1]$. This gives $\Delta^2 = 2s/\xi_1 - 2s/\xi + 2\ln\cosh(s/\xi_1)$.

It is easy to see that eqs. (42-48) give for large L $\rho_t(L) = \beta L - c'$, where $c' > c$. The segment resistance (45) increases with n, its lower limit at $n = 1$ is $\exp(f_1) - 1 = \exp(L/\xi) - 1$ while its upper limit at large n is $\int df\mathcal{P}(f)(\exp(f) - 1) = 0.5\,[\exp(2s/\xi_1) - 1]$. Physically, eq. (45) is the self-average of $\rho(s)$ in a single "typical" wire and therefore coincides with the ensemble average $0.5\,[\exp(2s/\xi_1) - 1]$ only at very large x, at which it involves also the tail of the resistance distribution. Otherwise $\rho(s) \ll 0.5\,[\exp(2s/\xi_1) - 1]$ and consequently $\beta_t(x) \ll \beta(x)$. Eventually, $\beta_t(x)$ converges towards β, but at much larger x as does the $\beta(x)$, so that $\rho_t(L) = \beta L - c'$ with the shift $c' \gg c$. In other words, the shift c' reflects a slowly converging process of the resistance self-averaging in a single wire.

We have also extracted $\rho_t(L)$ from eqs. (42-48) numerically. The result obtained for $L_\phi = 10.4$ μm is shown in Fig. 8 in a thin full line. It reasonably fits the decoherence model result shown in the thick full line, the fit further improves with increasing L_ϕ/ξ_1 (not shown). Note that for $L_\phi = 10.4$ μm the slope of the dotted line strongly differs from the slope of the thick full line, i.e., here the thick full line is quite far from the ohmic regime. It was not traced up to the ohmic regime, since the decoherence model of Sect. IV needs in this case too much computational time.

We have therefore applied the scheme (42-48), which is computationally fast. We have found that for $L_\phi = 10.4$ μm the typical resistance tends to be linear at $L > 10^{11}$ μm. We cannot offer any simple formula to explain this unprecedently large value, but it is interesting to compare Figs. 7 and 8. It can be seen that for $L_\phi = 1.5$, 3, and 5 μm the typical resistance becomes linear at those L at which the resistance dispersion becomes smaller than unity. Similarly, the dispersion for $L_\phi = 10.4$ μm would reach unity nearly at $L = 10^{11}$ μm.

The typical resistance should be much easier to measure than the mean resistance, because the dispersion of the variable f is small already in the coherent regime ($\Delta/\bar{f} \approx 1/\sqrt{L/\xi}$ for $L/\xi \gg 1$). In presence of decoherence the situation is favourable as well. Figure 9 shows the distributions $\mathcal{P}(f)$ obtained in the same simulation as the results of Fig. 5. It can be seen that the coherent distribution broadens with increasing L while the decoherence narrows the distribution as L exceeds L_ϕ. Eventually, at $L \gg L_\phi$ the decoherence drives the distribution towards a δ-function-like shape, i.e., the dispersion of f tends to be suppressed.

VI. SUMMARY AND DISCUSSION

We have modelled the effect of phase-breaking electron collisions on the electron transport in a disordered

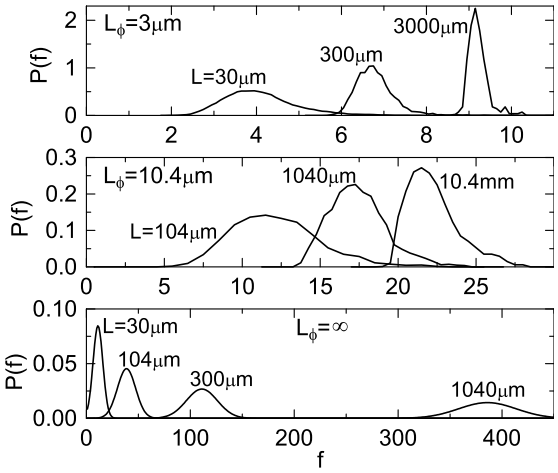

FIG. 9: Distribution of the variable $f = \ln(1+\rho)$, $\mathcal{P}(f)$, for various wire lengths L. Distributions in the coherent regime ($L_\phi = \infty$) are compared with the distributions perturbed by decoherence ($L_\phi = 3$ μm and $L_\phi = 10.4$ μm).

1D wire with single conducting channel. In our model the phase-breaking collisions effectively break the wire into independent segments, where each segment is a series resistor with coherent electron motion. We have modeled the segmentation as a stochastic process with a Poisson distribution of phase-breaking scattering times and we have evaluated the resistance of each segment microscopically from the Landauer formula.

The wire resistance as a function of the wire length L, coherence length L_ϕ, and localisation length ξ has been traced from the coherent regime at $L < L_\phi$ up to the incoherent one at $L \gg L_\phi$.

In the coherent regime the resistance fluctuates from wire to wire in accord with the DMPK resistance distribution, the typical resistance increases as $\exp(L/\xi)$, and the mean resistance increases as $\exp(2L/\xi)$. This is in agreement with the universal scaling theory.

As L exceeds L_ϕ, decoherence suppresses the resistance fluctuations and narrows the resistance distribution. As a result, at $L \gg L_\phi$ the mean resistance increases as $\beta L - c$ and the typical resistance as $\beta L - c'$, where β is the wire resistivity, c is a constant shift due to the decoherence near the source contact, and $c' \gg c$ is the shift related to the resistance self-averaging in a single wire.

As argued in Sect. IV, our model is in essence a simple phenomenological model of the e-e interaction mediated phase breaking, with the electron coherence length L_ϕ taken as a parameter. If compared with experiment, the model could help to determine the coherence length and also the localization length.

We have also discussed conditions necessary to measure our results in practice. The mean resistance might be measurable if L_ϕ does not exceed ξ more than about twice, otherwise the resistance fluctuations become too large to perform average over a sufficient number of wires. To average over millions of wires, one could perhaps spec-

ulate about a single wire with tunable disorder induced by an array of randomly biased gates. As to the typical resistance, one fortunately needs to average the variable $f = \ln(1+\rho)$, which is much easier to do.

We add a comment about the effect of finite temperature. We have implicitly assumed that the temperature is low enough for the contribution from the phonon mediated dephasing to be negligible. In the GaAs systems this is justified below ~ 1 K. However, we have used the zero-temperature formula (1), which may not be appropriate even for $T \ll \varepsilon_F/k_B$. We have therefore tested for $T \ll \varepsilon_F/k_B$, what happens if we replace the formula (1) by its temperature-dependent version.[39] We have found that in case of coherent transport the resistance distribution and the mean and typical resistance depend on the localisation length as at zero temperature, except that the localisation length is T-dependent.[40] The same has to hold for each coherent segment in a wire segmented by decoherence, thus the results presented in this paper are representative also for non-zero temperatures.

Our numerical simulations were performed in conditions characteristic of the GaAs quantum wire. In such wire the backscattering by disorder can be strong.[25] We have therefore also examined the effect of strong disorder on coherent transport. We have found deviations from universal scaling which differ from those reported for the Anderson model.[26]

Acknowledgments

P. V. was supported by a Marie Curie Fellowship of the Fifth Framework Programme of the European Community, contract no. HPMFCT-2000-00702. M.M. and P.V. were also supported by the VEGA grant no. 2/7201/21 and P. M. by the VEGA grant no. 2/7174/20.

APPENDIX A

The purpose of this Appendix is to analyze the coherent resistance of the chain of N identical obstacles and to derive the formulae (15), (16), and (17).

1. Mean resistance

The mean resistance (15) was derived by Landauer,[4] but it can be interesting to derive the same result in a more simple way. Consider two obstacles with resistances $\rho_a = R_a/(1-R_a)$ and $\rho_b = R_b/(1-R_b)$, where R_a and R_b are the reflection probabilities of the obstacles. The composite resistance of the two obstacles is[4]

$$\rho_2 = \frac{R_a + R_b + 2\sqrt{R_a R_b}\cos\phi}{(1-R_a)(1-R_b)}, \tag{A1}$$

where the phase $\phi = 2k_F a + \phi_0$, a is the interobstacle distance, and ϕ_0 is the (a-independent) phase shift due to the reflection by the obstacles . If one assumes that $a \gg 2\pi/k_F$, then ϕ changes rapidly with a and fluctuates at random from sample to sample as a fluctuates. In such case the ensemble average of eq. (A1) over the interobstacle distance is simply

$$\bar{\rho}_2 = \frac{1}{2\pi}\int_0^{2\pi} d\phi\, \rho_2. \tag{A2}$$

Inserting (A1) into (A2) one finds

$$\bar{\rho}_2 = \frac{R_a}{1-R_a} + \frac{1+R_a}{1-R_a}\,\frac{R_b}{1-R_b}. \tag{A3}$$

Consider now a chain of N identical obstacles, say impurities, where each obstacle is characterized by the reflection probability R_I. We follow the scaling procedure of Ref. 4: We identify R_a with the reflection probability of a single impurity added to the chain of $N-1$ impurities, we average over all phase differences in the chain of these $N-1$ impurities, and we identify $R_b/(1-R_b)$ with the mean resistance $\bar{\rho}_{N-1}$. Equation (A3) then gives

$$\bar{\rho}_N = \frac{\alpha-1}{2} + \alpha\,\bar{\rho}_{N-1}, \tag{A4}$$

where $\alpha = (1+R_I)/(1-R_I)$. We rewrite eq. (A4) as

$$\bar{\rho}_N = \frac{\alpha-1}{2}\left(1+\alpha+\alpha^2+\cdots+\alpha^{N-1}\right), \tag{A5}$$

which immediately gives eq. (15) as

$$\bar{\rho}(N) = \frac{\alpha-1}{2}\,\frac{\alpha^N-1}{\alpha-1} = \frac{1}{2}\left[\left(\frac{1+R_I}{1-R_I}\right)^N - 1\right]. \tag{A6}$$

2. Typical resistance

To obtain the typical resistance (17), one has to average over all possible configurations of impurity positions the variable $f_N = \ln(1+\rho_N)$, where N is the number of impurities. We start with two impurities and perform the ensemble average of $f_2 = \ln(1+\rho_2)$, where ρ_2 is given by the formula (A1). Similarly as in the preceding subsection, the ensemble average of f_2 can be written as

$$\bar{f}_2 = \frac{1}{2\pi}\int_0^{2\pi} d\phi\, \ln\left[\frac{1+R_aR_b+2\sqrt{R_aR_b}\cos\phi}{(1-R_a)(1-R_b)}\right], \tag{A7}$$

which gives

$$\bar{f}_2 = \ln\left(\frac{1}{1-R_a}\right) + \ln\left(\frac{1}{1-R_b}\right). \tag{A8}$$

Applying the scaling procedure of the preceding subsection one easily obtains the recursion relation

$$\bar{f}_N = \ln\left(\frac{1}{1-R_I}\right) + \bar{f}_{N-1}, \tag{A9}$$

which gives

$$\bar{f}_N = N \ln\left(\frac{1}{1-R_I}\right). \tag{A10}$$

Finally, inserting eq. (A10) into the definition $\rho_t(N) = e^{\bar{f}_N} - 1$ we obtain the typical resistance (17).

3. Mean squared resistance

Now we derive eq. (16), i.e., we calculate the mean value $\bar{\rho^2}(N)$ of the squared resistance $\rho^2(N)$. We start again with two impurities and calculate the quantities

$$\bar{X}_2 = \frac{1}{2\pi}\int_0^{2\pi} d\phi\ (\rho_2)^2\,, \tag{A11a}$$

$$\bar{Y}_2 = \frac{1}{2\pi}\int_0^{2\pi} d\phi\ (1+\rho_2)^2\,, \tag{A11b}$$

and

$$\bar{Z}_2 = \frac{1}{2\pi}\int_0^{2\pi} d\phi\, 2\rho_2\,(1+\rho_2)\,. \tag{A11c}$$

where ρ_2 is given by (A1). We obtain a set of equations

$$\bar{X}_2 = Y_a X_b + X_a Y_b + Z_a Z_b, \tag{A12a}$$

$$\bar{Y}_2 = X_a X_b + Y_a Y_b + Z_a Z_b, \tag{A12b}$$

$$\bar{Z}_2 = Z_a X_b + Z_a Y_b + (X_a + Y_a + Z_a)\, Z_b, \tag{A12c}$$

where $X_a = [R_a/(1-R_a)]^2$, $Y_a = 1/(1-R_a)^2$, $Z_a = 2R_a/(1-R_a)^2$, and X_b, Y_b, and Z_b are given analogously.

We apply the scaling procedure of subsection 1 and rewrite eqs. (A12) into the recursion vector form

$$\begin{pmatrix} \bar{X}_N \\ \bar{Y}_N \\ \bar{Z}_N \end{pmatrix} = \mathcal{A} \begin{pmatrix} \bar{X}_{N-1} \\ \bar{Y}_{N-1} \\ \bar{Z}_{N-1} \end{pmatrix} = \mathcal{A}^{N-1} \begin{pmatrix} X_I \\ Y_I \\ Z_I \end{pmatrix}, \tag{A13}$$

where

$$\mathcal{A} = \begin{pmatrix} Y_I & X_I & Z_I \\ X_I & Y_I & Z_I \\ Z_I & Z_I & X_I + Y_I + Z_I \end{pmatrix}. \tag{A14}$$

Equations (A13) can be solved by expanding the vector (X_I, Y_I, Z_I) as a linear combination of eigenvectors of the matrix $\mathcal{A}$. We obtain

$$\bar{X}_N = -\frac{1}{2}\lambda_1^N + \frac{1}{3}\lambda_2^N + \frac{1}{6}\lambda_3^N, \tag{A15}$$

where λ_1, λ_2, and λ_3 are the eigenvalues of $\mathcal{A}$, namely $\lambda_1 = Y_I - X_I$, $\lambda_2 = X_I + Y_I - Z_I$, and $\lambda_3 = X_I + Y_I + 2Z_I$. In terms of R_I we have $\lambda_1 = (1+R_I)/(1-R_I)$, $\lambda_2 = 1$, and $\lambda_3 = 1 + 6R_I/(1-R_I)^2$. Inserting these expressions into eq. (A15) we obtain the equation

$$\bar{\rho^2}(N) = \frac{1}{3} - \frac{1}{2}\left(\frac{1+R_I}{1-R_I}\right)^N + \frac{1}{6}\left(1 + \frac{6R_I}{(1-R_I)^2}\right)^N, \tag{A16}$$

which is identical with eq. (16).

---

* Electronic address: elekmoso@savba.sk

[1] C. Weisbuch and B. Vinter, *Quantum Semiconductor Structures: Fundamentals and Applications* (Academic Press, London, UK, 1991).

[2] B. J. van Wees, H. van Houten, C. W. J. Beenakker, J. G. Williamson, L. P. Kouwenhoven, D. van der Marel, and C. T. Foxon, Phys. Rev. Lett. **60**, 848 (1988); D. A. Wharam, T. J. Thornton, R. Newbury, M. Pepper, H. Ahmed, J. E. F. Frost, D. G. Hasko, D. C. Peacock, D. A. Ritchie, and G. A. C. Jones, J. Phys. C **21**, L209 (1988).

[3] S. Tarucha, T. Honda, and T. Saku, Solid State Commun. **94**, 413 (1995).

[4] R. Landauer, Philos. Mag. **21**, 863 (1970).

[5] R. Landauer, in *Analogies in Optics and Micro Electronics*, edited by W. van Haeringen and D. Lenstra (Kluwer Academic Publishers, Dordrecht, 1990), pp. 243–258.

[6] S. Datta, *Electronic Transport in Mesoscopic Systems* (Cambridge University Press, Cambridge, UK, 1995).

[7] D. L. Maslov and M. Stone, Phys. Rev. B **52**, R5539 (1995); V. V. Ponomarenko, Phys. Rev. B **52**, R8666 (1995).

[8] N. F. Mott and W. D. Twose, Adv. Phys. **10**, 107 (1961).

[9] R. E. Borland, Proc. Phys. Soc. **78**, 926 (1961).

[10] N. F. Mott, *Metal-Insulator Transition* (Taylor and Francis, London, England, second edition, 1990).

[11] P. W. Anderson, D. J. Thouless, E. Abrahams, and D. S. Fisher, Phys. Rev. B **22**, 3519 (1980).

[12] C. W. J. Beenakker, Rev. Mod. Phys. **69**, 731 (1997).

[13] K. A. Matveev, D. Yue and L. I. Glazman, Phys. Rev. Lett. **71**, 3351 (1993); D. Yue, L. I. Glazman, and K. A. Matveev, Phys. Rev. B **49**, 1966 (1994).

[14] B. L. Altshuler and A. G. Aronov, in *Electron-Electron Interactions in Disordered Systems*, edited by A. L. Efros and M. Pollak (Elsevier Science Publishers B. V., 1985).

[15] D. S. Golubev and A. D. Zaikin, Phys. Rev. B **62**, 14061 (2000).

[16] P. Mohanty, Physica B **280**, 446 (2000).

[17] M. E. Gershenson, Ann. Phys. (Leipzig) **8**, 7-9, 559 (1999).
[18] M. Büttiker, Phys. Rev. B **33**, 3020 (1986).
[19] P. A. Mello, Y. Imry, and B. Shapiro, Phys. Rev. B **61**, 16570 (2000).
[20] O. N. Dorokhov, Zh. Eksp. Teor. Fiz **98**, 646 (1990); Sov. Phys. JETP **71**, 360 (1990).
[21] D. L. Shepelyansky, Phys. Rev. Lett. **73**, 2607 (1994).
[22] Yu. M. Sirenko, V. Mitin, and P. Vasilopoulos, Phys. Rev. B **50**, 4631 (1994).
[23] M. Moško and V. Cambel, Phys. Rev. B **50**, 8864 (1994).
[24] B. Shapiro, Philos. Mag. B **56**, 1031 (1987).
[25] M. Moško and P. Vagner, Phys. Rev. B **59**, R10445 (1999).
[26] K. M. Slevin and J. B. Pendry, J. Phys: Cond. Matt. **2**, 2821 (1990).
[27] Equation (6) was first obtained by V. I. Melnikov [Soviet Phys. Solid St. **23**, 444 (1981)] and a formally different version by A. Abrikosov [Solid St. Commun. **37**, 997 (1981)]. Derivations beyond the single channel limit are due to O. N. Dorokhov, JETP Letters **36**, 318 (1982), and due to P. A. Mello, P. Pereyra, and N. Kumar, Ann. Phys. (NY) **181**, 290 (1988).
[28] P. Erdös and R. C. Herndon, Adv. Phys. **31**, 65 (1982); W. W. Lui and M. Fukuma, J. Appl. Phys **60**, 1555 (1986); Y. Ando and T. Itoh, J. Appl. Phys **61**, 1497 (1987); J. Flores, P. A. Mello, and G. Monsiváis, Phys. Rev. B **35**, 2144 (1987).
[29] P. Markoš and B. Kramer, Ann. Phys. **2**, 339 (1993).
[30] To assume that each e-e collision completely randomizes the electron phase is a simplification. Such simplification seems to works reasonably say in metalic quasi-1D wires, as shown by A. B. Gougham, F. Pierre, H. Pothier, D. Esteve, and N. O. Birge, cond-mat/9912137 (1999), but whether it works in a single 1D channel is an unresolved problem. The phase breaking might also be due to the gradual accumulation of phase during many collisions involving small energy exchange, which is not considered in our model
[31] B. Kramer and J. Mašek, Z. Phys. B **76**, 457 (1989).
[32] M. E. Farrell, M. F. Bishop, N. Kumar, and W. E. Lawrence, Phys. Rev. B **42**, 3260 (1990).
[33] D. Kaufman, Y. Berk, B. Dwir, A. Rudra, A. Palevski, and E. Kapon, Phys. Rev. B **59**, R10433 (1999).
[34] M. Blencowe and A. Shik, Phys. Rev. B **54**, 13899 (1996), presented formulae similar to eqs. (33) and (35), however they inserted for $\rho(s)$ the typical coherent resistance rather than the mean coherent resistance. According to Sect. IV the typical coherent resistances of individual segments should not be added ohmically.
[35] For example, occurence of the segment $s = 0.7L$ in the wire of length L implies that occurence of the segments $s > L - 0.7L$ in the same configuration of segments is not allowed. Eqs. (37) and (34) ignore this problem.
[36] The formula $d(L)/\sqrt{n_w}$ is applicable if $d(L) \propto 1/\sqrt{L}$, which is the case in presence of decoherence. In the coherent regime it is not applicable if $L \gg \xi$ (according to our numerical experience if $d_{coh}(L) > 10$), because for $L \gg \xi$ the $d_{coh}(L)$ is completely dominated by the tail of the resistance distribution.
[37] A. Yacoby, H. L. Stormer, N. S. Wingreen, L. N. Pfeiffer, K. W. Baldwin, and K. W. West, Phys. Rev. Lett. **77**, 4612 (1996).
[38] R. dePicciotto, H. L. Stormer, L. N. Pfeiffer, K. V. Baldwin, and K. W. West, Nature **411**, 51 (2001).
[39] M. Büttiker, Y. Imry, R. Landauer, and S. Pinhas, Phys. Rev. B **31**, 6207 (1985).
[40] This finding means that opening of the energy channels in the vicinity of the Fermi energy channel effectively enhances the number of samples with different disorder but does not change the statistics. The finding seems to be consistent with the ergodic hypothesis by B. L. Altshuler, V. E. Kravtsov and I. V. Lerner, JETP Letters **43**, 441 (1986), albeit these authors addressed the regime of universal conductance fluctuations.